Solid-State Electronics 62 (2011) 138–141

Contents lists available at ScienceDirect

Solid-State Electronics

journal homepage: www.elsevier.com/locate/sse

Study of Shubnikov–de Haas oscillations and measurement of hole effective mass in compressively strained $In_XGa_{1-X}Sb$ quantum wells

Aneesh Nainani [a,*], Toshifumi Irisawa [a], Brian R. Bennett [b], J. Brad Boos [b], Mario G. Ancona [b], Krishna C. Saraswat [a]

[a] Center for Integrated Systems, Department of Electrical Engineering, Stanford University, Stanford, CA 94305, USA
[b] Naval Research Laboratory, Washington, DC 20375, USA

ARTICLE INFO

Article history:
Received 26 November 2010
Received in revised form 25 March 2011
Accepted 4 April 2011
Available online 4 May 2011

The review of this article was arranged by Prof. S. Cristoloveanu

Keywords:
Field effect transistors
III-V CMOS
III-V pMOSFET
Shubnikov-de Haas
Hole effective mass
Cyclotron resonance
III-V

ABSTRACT

$In_XGa_{1-X}Sb$ has the highest hole mobility amongst all III–V semiconductors which can be enhanced further with the use of strain. The use of confinement and strain in $In_XGa_{1-X}Sb$ quantum wells lifts the degeneracy between the light and heavy hole bands which leads to reduction in the hole effective mass in the lowest occupied band and an increase in the mobility. We present magnetotransport measurements on compressively strained $In_XGa_{1-X}Sb$ and GaSb quantum wells. Hall-bar and Van de Pauw structures were fabricated and Shubnikov–de Haas oscillations in the temperature range of $T = 2$–10 K for magnetic fields of $B = 0$–9 T were measured. The reduction of effective hole mass with strain was quantified. These results are in excellent agreement with modeling results from band structure calculations of the effective hole mass in the presence of strain and confinement.

© 2011 Elsevier Ltd. All rights reserved.

Recently, there has been significant interest in the use of III–V materials to replace Si as channel material for future CMOS technology nodes. High electron mobility has been demonstrated in *n*-MOSFET devices using $In_XGa_{1-X}As$ channel [1]. In the meantime progress has also been made towards improving the hole mobility in III–V's which has been less promising in the past in comparison to strained-Si. Biaxially strained $In_XGa_{1-X}As$ quantum wells have been studied to enhance hole mobility with maximum reported room-temperature hole mobility in the range of 300–400 cm^2/Vs [2,3]. Sb-based channels appear attractive candidates for III–V PMOS because of their high bulk mobility. Recently, we demonstrated high hole mobility in Sb-based quantum wells with biaxial compressive strain [4,5]. Hole mobility of 1200 cm^2/Vs in strained $In_XGa_{1-X}Sb$ quantum well [4], and 1350 cm^2/Vs in strained GaSb quantum well [5] was obtained (at sheet charge of $\sim 1 \times 10^{12}/cm^2$). One of the most important consequences of the presence of strain and confinement in these quantum wells is the lifting of the degeneracy of the light and heavy hole bands, which results the reduction of the hole effective mass in the lowest occupied band and an increase in mobility [6].

Study of the Shubnikov–de Haas oscillations in the resistivity of a two-dimensional hole gas in a quantum well along with Hall measurements can yield important information about its characteristics, such as the effective mass of the charge carriers, number of bands occupied, spin degeneracy, quantum scattering time, etc. In this letter we present a systematic study of Shubnikov–de Haas oscillations in compressively strained quantum wells with (A) $In_XGa_{1-X}Sb$ and (B) GaSb channels. Biaxial compression, which has been predicted to be optimum for hole mobility enhancement [7], is introduced into the quantum well by engineering the lattice mismatch between the channel and barrier material during MBE growth. Fig. 1 shows a cartoon of the different layers in the stack and cross section TEM image around the channel region. A modulation doping scheme using Be is employed. For the GaSb channel devices the $AlAs_XSb_{1-X}$ barrier is grown as superlattice of AlAs and AlSb (Fig. 1) [5]. Details on the growth are available in Refs. [5,6]. Percentage of strain in the channel layers was calculated using X-ray diffraction (XRD) analysis [4,5].

Hall-bar and Van der Pauw structures were fabricated for magnetotransport measurements [8]. A low frequency lock-in amplifier technique was used to avoid any interference from the power line. The temperature was varied from 2 K to 300 K and magnetic field up to 9 T was applied. Details on samples studied

* Corresponding author. Tel.: +1 6505212623.
E-mail address: nainani@stanford.edu (A. Nainani).

0038-1101/$ - see front matter © 2011 Elsevier Ltd. All rights reserved.
doi:10.1016/j.sse.2011.04.005

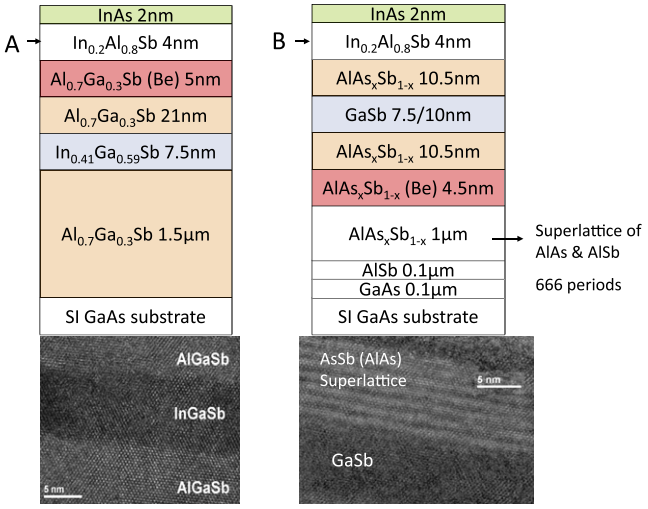

Fig. 1. Cross-section showing the layer details in a quantum well heterostructure with (A) $In_XGa_{1-X}Sb$ and (B) GaSb channel. The $AlAs_XSb_{1-X}$ layers are composed of AlSb/AlAs short-period superlattices. Also shown are high resolution TEM images around the channel region.

in this paper and their mobility at 300 K and 2 K measured using Hall measurements are given in Table 1. For samples A1, A2 and B1, high low-temperature mobility in the range 4400–5000 cm^2/Vs is obtained. For samples A3 and B2 the target strains were 1.8% and 1.48%, respectively; however, relaxation of strain occurred in these samples due to channel width exceeding the critical thickness. This results in the degradation in the room-temperature mobility and much higher degradation in the low-temperature mobility value in A3, B2 (Table 1). For Shubnikov–de Haas oscillations to occur the required condition is $\omega_c\tau* \gg 1$ where $\tau*$ is the quantum (single-particle) relaxation time and $\omega_c = eB/m^*$ is the cyclotron frequency with m^* being the hole effective mass and B is the magnetic field. Thus high low-temperature mobility implying high relaxation time is critical for observation of Shubnikov–de Haas oscillations within the given field/temperature range fixed by the experimental setup.

Fig. 2a plots the scan of sheet resistance with magnetic field (0–9 T) for sample A1 with mobility of 4500 cm^2/Vs and sheet charge $1.3 \times 10^{12}/cm^2$ at 2 K. An oscillatory behavior can clearly be seen superimposed on a parabolic dependence with magnetic field. The oscillatory behavior is plotted vs. B in Fig. 2b for various temperatures, removing the parabolic dependence, which occurs due to hole–hole interactions [9]. No signature of Zeeman splitting is seen in the studied B field range. Oscillations are periodic with $1/B$, a fast Fourier transform (Fig. 2b, inset) on the data shows that the oscillations are harmonic with a single frequency implying occupancy of only the lowest energy hole subband. The frequency of the oscillations in the longitudinal resistance as a function of the inverse magnetic field is related to the electron concentration as $n_s = g_s g_v e/[h\Delta(1/B)]$ where g_s and g_v are the spin and valley degeneracies, h is Planck's constant. Using the carrier density obtained from Hall measurements at 2 K (Table 1), the product of valley and spin degeneracy g_s and g_v can be determined from the period of the oscillations. It was found to be in the range 4.0–4.1 for all samples in satisfactory agreement with the expected value of 4.

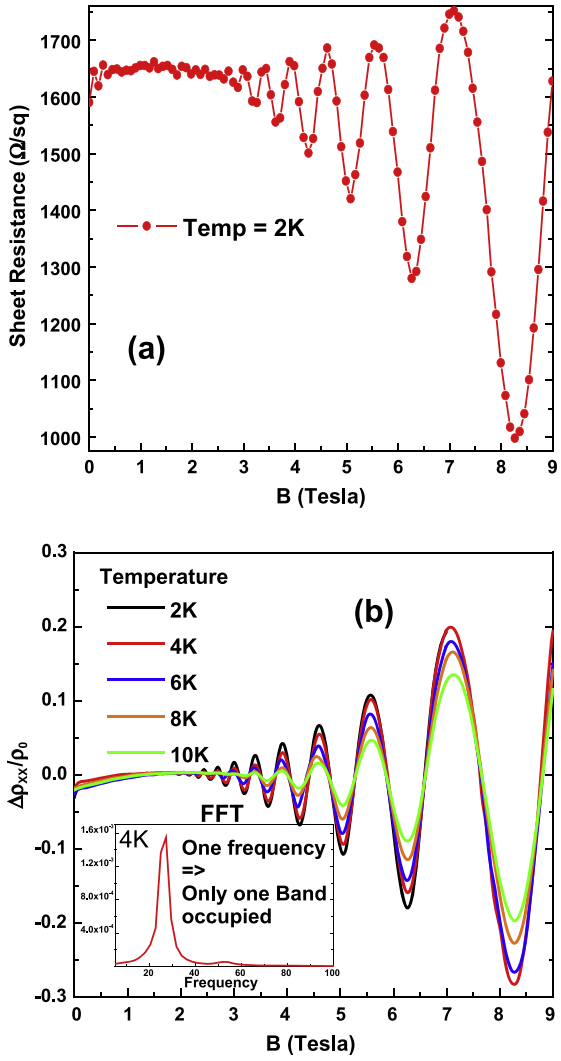

Fig. 2. (a) Shubnikov–de Haas oscillations seen in the sheet resistance at 2 K (sample A1). (b) The oscillatory behavior is plotted for various temperatures removing the parabolic dependence due to hole–hole interaction. The oscillations are periodic vs. 1/B, with a single frequency as verified from taking a fast Fourier transform on the data (inset b).

The peak amplitude of the oscillations ($\Delta\rho_p$) can be described using the Ando formula [10]

$$\frac{\Delta\rho_p}{\rho_0} = R_S V \frac{\xi}{\sinh\xi}\exp\left(\frac{-\pi}{\omega_c\tau_q}\right)$$

Table 1
Details on the samples studied. Mobility at 300 K and mobility and sheet charge (N_S) at 2 K measured using Hall measurements are listed. Strain is calculated using XRD analysis [5–6].

Sample	Channel (thickness (Å))	Barrier	Strain (%)	μ_{Hall} (300 K) ($cm^2 V^{-1} s^{-1}$)	μ_{Hall} (2 K) ($cm^2 V^{-1} s^{-1}$)	N_S (2 K) (cm^{-2})
A1	$In_{0.41}Ga_{0.59}Sb$ (75)	$Al_{0.7}Ga_{0.3}Sb$	1.8	960	4500	1.3×10^{12}
A2	$In_{0.41}Ga_{0.59}Sb$ (75)	AlSb	1.9	900	5000	0.94×10^{12}
A3	$In_{0.41}Ga_{0.59}Sb$ (125)	$Al_{0.7}Ga_{0.3}Sb$	1.8[a]	621	2210	1.0×10^{12}
B1	GaSb (75)	$AlAs_{0.219}Sb_{0.781}$	1.06	880	4400	1.5×10^{12}
B2	GaSb (75)	$AlAs_{0.238}Sb_{0.762}$	1.48[a]	600	1500	1.27×10^{12}

[a] For samples A3 and B2 the ideally targeted value of strain is listed. Mobility degradation is observed due to strain relaxation in these samples due to channel width exceeding the critical layer thickness.

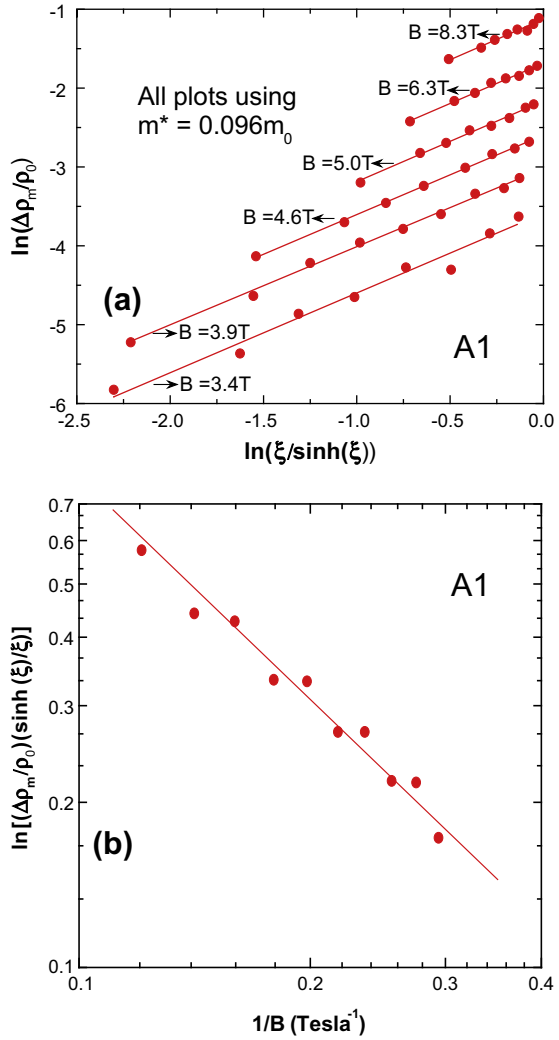

Fig. 3. (a) Effective hole mass is calculated using the temperature dependence of the oscillations as the value for which a gradient of unity is obtained in the plot of $\ln\left(\frac{\Delta\rho_p}{\rho_0}\right)$, vs. $\ln\left(\frac{\xi}{\sinh\xi}\right)$. (b) Dingle plot: Slope of line is $-\pi\alpha/\mu$ where α is the ratio τ/τ_q of the transport time τ to the quantum lifetime τ_q.

where ρ_0 is the resistance at zero B, τ_q is the quantum lifetime, $\xi = 2\pi^2 kT/\hbar\omega_c$ and $\omega_c = eB/m^*$. The prefactor R_s, is associated with Zeeman splitting while V is usually set equal to 4. R_s, and V are assumed to be independent of magnetic field and temperature in which case they are not involved in the following analysis. Fig. 3a plots $\ln\left(\frac{\Delta\rho_p}{\rho_0}\right)$, vs. $\ln\left(\frac{\xi}{\sinh\xi}\right)$ in the temperature range 2–10 K, for various values of B at which the peak occurs. m^* is calculated as the value for which a gradient of unity is obtained in each sample. Table 2 summarizes the m^* values for different samples. The value of m^* is found to independent of the selection of the magnetic field at which the oscillation peak occurs, implying the band is parabolic in the measured sheet charge range ($\sim$0.94–1.8 $\times$ 10^{12}/cm^2). No oscillations were seen for the samples in which strain relaxation had occurred (A3, B2) and which exhibit poor low-temperature mobility.

In Fig. 3b, the Dingle plot is shown for the data of sample A1. Here, $\ln\left(\frac{\Delta\rho_m}{\rho_0}\frac{\sinh\xi}{\xi}\right)$ is plotted against the reciprocal field ($1/B$). The data fits well a straight line for various temperatures, confirming that the experimentally determined m^* is also independent of temperature. Noting that the gradient of the line is $-\pi\alpha/\mu$ where α is the ratio τ/τ_q of the transport time τ to the quantum lifetime τ_q and μ is the Hall mobility, we obtain α in the range of 0.9–1.0 for all samples. This value should be compared with Gold's predictions of $\alpha = 1$ for scattering by interface charge and $\alpha = 0.67$ for short-range interface roughness scattering [11], which suggests that the low-temperature mobility in our samples is limited by a combination of scattering by interface charge and interface roughness scattering at the $In_XGa_{1-X}Sb/Al_XGa_{1-X}Sb$ interface.

To understand the experimental findings, the measured effective hole mass was compared with those derived from the band structure calculated using the eight band *k.p* approach [7]. Effect of strain was incorporated using the 8 $\times$ 8 strain Hamiltonian in Ref. [12]. To model the band structure in the quantum well and calculate the effective mass we closely follow the approach in Ref. [13]. Table 2 summarizes the results from the modeling along with the results from Shubnikov–de Haas oscillations. Experimental results are found to be in good agreement with the value from the modeling. Table 2 also lists the value of m^* from *k.p* modeling when the light and heavy hole bands become completely uncoupled i.e. $m^* = 1/(\gamma_1 + \gamma_2)$ where γ_1, γ_2 are the Luttinger parameters. We observe that for $In_XGa_{1-X}Sb$ sample A2 with 1.9% biaxial strain the measured m^* of 0.094 m_0 is close to the value of 0.06 m_0 when the bands become uncoupled. For GaSb samples there is room for further reduction in m^* if more than 1.06% biaxial compression could be introduced without strain relaxation, meaning the mobility in GaSb quantum well can be improved further with strain. To further support our experimental findings, the effective hole mass in sample A2 was measured using cyclotron resonance and found to be 0.096 m_0 is very good agreement with the results from Shubnikov–de Haas measurements and modeling.

In summary, magnetotransport measurements have been performed on compressively strained $In_{0.41}Ga_{0.59}Sb$ and GaSb quantum wells in the temperature range 2–300 K and magnetic field up to 9 T. High hole mobility in these samples makes observation of Shubnikov–de Haas oscillations possible. Study of these oscillations reveals that only the lowest energy hole subband is occupied in the measured sheet charge range (Table 1), and the low-temperature mobility is limited by large angle scattering mechanisms. Effective hole mass extracted from the temperature dependence of the oscillations is found to be in good agreement with results from *k.p* modeling. Presence of strain and confinement in these samples leads to reduction of hole effective mass to minimum of 0.094 m_0, which comes close to numbers typically associated with electron effective mass in III–V materials.

Table 2
Summary of hole effective mass (m^*) with strain: extracted value from Shubnikov–de Haas oscillations (SdH), results from band structure modeling (*k.p*) and verification with cyclotron resonance (CR).

Sample	Channel (Å)	Strain (%)	μ_{Hall} (2 K) (cm^2 V^{-1} s^{-1})	m^* (m_0)	m^* when no coupling (m_0)
A1	$In_{0.41}Ga_{0.59}Sb$ (75)	1.8	4500	0.099 (SdH), 0.09 (*k.p*)	m^*_{min} : 0.06($k.p = 1/(\gamma_1+\gamma_2)$
A2	$In_{0.41}Ga_{0.59}Sb$ (75)	1.9	5000	0.094 (SdH), 0.085 (*k.p*), 0.096 (CR)	
A3	$In_{0.41}Ga_{0.59}Sb$ (125)	1.8[a]	2213	Strain relaxation: no oscillations	
B1	GaSb (75)	1.06	4400	0.12 (SdH), 0.10 (*k.p*)	m^*_{min} : 0.07($k.p = 1/(\gamma_1+\gamma_2)$
B2	GaSb (75)	1.48[a]	1500	Strain Relaxation: no oscillations	

[a] Target value of strain.

Acknowledgments

This work was partially supported by the Office of Naval Research. A. Nainani would like to thank Intel Corporation for a PhD fellowship and Rick Pam for providing the Agilent 4155C used in this research.

References

[1] Radosavljevic M, Chu-Kung B, Corcoran S, Dewey G, Hudait MK, Fastenau JM, et al. IEDM Tech Dig 2009:319.
[2] Drummond TJ, Zipperian TE, Fritz IJ, Schirber JE, Plut TA. Appl Phys Lett 1986;49:461.
[3] Kusters AM, Kohl A, Sommer V, Muller R, Heime K. IEEE Trans Electron Dev 1993;40:2164.
[4] Bennett 4BR, Ancona MG, Boos JB, Shananbrook BV. Appl Phys Lett 2007;91:042104.
[5] Bennett BR, Ancona MG, Boos JB, Canedy CB, Khan SA. J Crys Growth 2008;311:47–53.
[6] Klem JF, Lott JA, Schirber JE, Kurtz SR, Lin SY. J Electron Mater 1993;22:315.
[7] Nainani A, Kim D, Krishnamohan T, Saraswat K. In: Proceedings of SISPAD 2009; 2009. p. 47–50
[8] Schroder DK. 3rd ed. New York: John Wiley & Sons; 2005 [Chapter 8].
[9] Houghton A, Senna JR, Ying SC. Phys Rev B 1982;25:2196.
[10] Ando T, Fowler AB, Stern F. Rev Mod Phys 1982;54:437.
[11] Gold A. Phys Rev B 1988;38:10798.
[12] Bahder TB. Phys Rev B 1990;41:11992.
[13] Liu YX, Ting DZ-Y, McGill TC. Phys Rev B 1996;54:5675.